Finite-Time LPV Analysis of a Vision Based Landing System with Anti-Windup Augmentation

Jean-Marc Biannic, Laurent Burlion, Sophie Tarbouriech

Finite-Time LPV Analysis of a Vision Based Landing System with Anti-Windup Augmentation

Jean-Marc Biannic * **Laurent Burlion** * **Sophie Tarbouriech** **

* *ONERA-Toulouse (e-mail: biannic@onera.fr).*
University of Toulouse, France.

** *LAAS-CNRS*
University of Toulouse, France.

Abstract: In contrast to standard ILS-based landing control systems, vision-based strategies rely on specific measures that introduce non-linearities into the control laws. Moreover, during the landing phase high gains are often used to improve performances at the expense of stability which is then degraded. This is not much an issue since both final approach and flare segments are short-time maneuvers. However, high gains induce saturations which in turn lead to performances degradation. For these reasons, vision-based landing systems design and tuning require a specific attention which generally involves a time-consuming trial-and-error process. The latter could certainly be fasten and improved with the help of adapted analysis tools providing a reliable estimate of the finite-time performance level of the aforementioned saturated nonlinear closed-loop system. As observed in Biannic and Burlion (2017), it can be rewritten as a saturated Linear Parameter Varying (LPV) system for which many tools exist or can be extended. In this contribution, original discrete-time extensions are then proposed to characterize finite-time performance indexes for a vision-based landing system including an anti-windup device.

Keywords: Saturated systems, LPV systems, Finite-time analysis, vision-based control.

1. INTRODUCTION

Many airports are now equipped with Instrument Landing Systems (ILS) that significantly secure the landing phase in poor visibility conditions. However, the installation and maintenance of such equipment remain very expensive and is not always available. This is generally the case for small airports and especially for unprepared runways, which could, however, be used for emergency landings. In such cases (but not only) vision landing systems offer an attractive and inexpensive alternative. This is why such solutions have been studied in recent years (see for example: Bourquardez and Chaumette (2007); Azinheira and Rives (2008); Le Bras et al. (2009); Huh and Shim (2010)) and are currently being explored further by the aviation industry (see: Gibert and Puyou (2013); Dickmanns et al. (2015); Gibert et al. (2015)). Despite the very promising results obtained in simulations with IBVS (Image-Based Visual Servoing) or PBVS (Pose-Based Visual Servoing) or a combination of both, there are still some obstacles before these solutions can be used on commercial aircraft:

- thorough evaluations under real conditions must be carried out using "true" images captured from video sequences,
- the computational requirements must be carefully evaluated to check compatibility with on-board computers,
- a specific validation process must be defined for certification needs.

Based on the Finite-Time-Stability (FTS) concept for Linear Time Varying (LTV) systems (see Dorato (1961); Garcia et al. (2009)), preliminary results of Biannic and Burlion (2017) are extended here to provide reliable estimates of finite-time performance indexes for saturated parameter-varying systems. As was indeed clarified in Biannic and Burlion (2017), unlike ILS-based controllers, the vision-based landing control system introduces in the closed-loop plant a specific nonlinearity that can be replaced by a varying parameter which constantly grows during the landing phase until flare is activated. Moreover, during this critical phase, high gains tend to be used to maintain the aircraft on its nominal path with a good accuracy despite perturbations. This however induces saturations. The development of specific tools for analysis of saturated LPV systems along given parametric trajectories is then very useful in the context of vision-based control assessment and improvement. The solution proposed in Biannic and Burlion (2017) provides an initial response without however taking into account the finite-time horizon property of the problem which is essential here. The proposed extension detailed in this paper is based on a discrete-time reformulation as described in

⋆ This work was partly supported by ANR VISIOLAND project ANR-13-CORD-0012 dedicated to VISIOn based aircraft LANDing techniques

section 2. Next, the main performance analysis results are detailed in section 3 and applied to the evaluation of a vision-based landing system in section 4. The interest of an anti-windup device is clearly demonstrated there. Finally concluding comments and future directions are proposed in section 5.

2. A BOUNDED-HORIZON TIME-VARYING ANALYSIS PROBLEM WITH SATURATIONS

2.1 System description & preliminary analysis

As detailed in Biannic and Burlion (2017), we focus on the glide slope phase illustrated in Figure 1 during which the autopilot system must maintain a constant slope $\gamma_0 = -3^o$ and a constant airspeed V despite external perturbations.

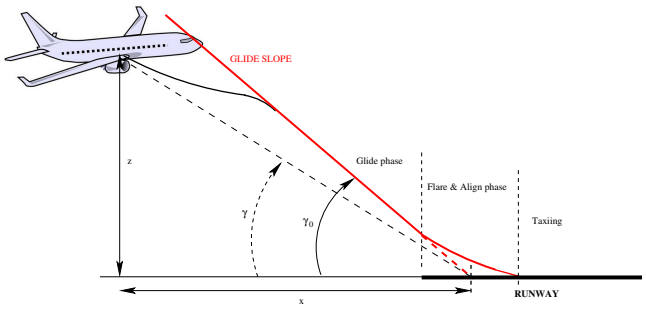

Fig. 1. Landing phases

It is assumed that an inner-loop controller has been defined to track the vertical acceleration $\ddot{z}$ as long as it remains bounded ($|\ddot{z}| \leq L_a$). Moreover, under low wind conditions, the horizontal speed verifies the approximation $\dot{x} \approx V$, so that the studied open-loop system reduces to:

$$\begin{cases} \dot{x} = V \\ \ddot{z} = \text{sat}_{L_a}(u) \end{cases} \tag{1}$$

In a vision-based landing context (see for example Gibert et al. (2015) for further details) this system is initially controlled by a nonlinear proportional-derivative controller:

$$u_0 = k_p \left(\frac{z}{x} - \gamma_0 \right) - k_d(\dot{z} - \gamma_0 V) \tag{2}$$

whose gains $k_p > 0$ and $k_d > 0$ are tuned such that, at the beginning of the glide phase, the system is well-damped and the desired slope is rapidly reached. The non-linearity $\gamma_m = z/x$ is introduced by the visual features. After a variable change $\xi_1 = z - \gamma_0 x$ and $\xi_2 = \Delta v_z = \dot{z} - \gamma_0 V$, one obtains a linear time-varying (LTV) system:

$$\begin{cases} \dot{\xi}_1 = \xi_2 \\ \dot{\xi}_2 = \text{sat}_{L_a}\left(-\lambda(t)\xi_1 - k_d\xi_2\right) \end{cases} \tag{3}$$

with:

$$\lambda(t) = -k_p/x(t) \tag{4}$$

The above system has been studied in Biannic and Burlion (2017) with $k_d = 0.3$ and an increasing parameter $\lambda(t)$ such that:

$$\lambda(t) \in [0.1\,,\ 0.5]\,, \quad \dot{\lambda}(t) = 0.35\,\lambda(t)^2 \tag{5}$$

which corresponds to the final approach phase starting approximately $2000\,m$ before the runway threshold with a constant speed $V = 70\,ms^{-1}$. This preliminary study has revealed that the combined effects of the parametric variations with the saturated acceleration were responsible for a severe performance degradation.

2.2 Model-Recovery Anti-Windup (MRAW) design

In this section, it is proposed to enhance the control law (2) with an anti-windup augmentation defined as follows:

- if λ were known, a conventional model-recovery anti-windup scheme Zaccarian and Teel (2011) would consist in choosing:

$$u = -\lambda(\xi_1 - \xi_{1,aw}) - k_d(\xi_2 - \xi_{2,aw}) + u_{aw} \tag{6}$$

$$\begin{cases} \dot{\xi}_{1,aw} = \xi_{2,aw} \\ \dot{\xi}_{2,aw} = \text{sat}_{L_a}(u) - (u - u_{aw}) \\ u_{aw} = -k_{1,aw}.\xi_{1,aw} - k_{2,aw}.\xi_{2,aw} \end{cases} \tag{7}$$

- in the case λ is unknown (which is our case), Burlion and de Plinval (2017) used an estimate $\hat{\lambda}$ in its anti-windup scheme and proved that the closed-loop system was stable using a well-chosen Lyapunov function. Here, we propose to use a more intuitive anti-windup loop which uses a constant value λ_a. Doing so, the anti-windup design is simple but one needs new analysis techniques (especially in the finite-time case) to guarantee that the closed-loop system remains stable.

We thus consider the following control law:

$$u = -\lambda\xi_1 + \lambda_a\xi_{1,aw} - k_d(\xi_2 - \xi_{2,aw}) + u_{aw} \tag{8}$$

with

$$\begin{cases} \dot{\xi}_{1,aw} = \xi_{2,aw} \\ \dot{\xi}_{2,aw} = \text{sat}_{L_a}(u) - (u - u_{aw}) \\ u_{aw} = -k_{1,aw}.\xi_{1,aw} - k_{2,aw}.\xi_{2,aw} \end{cases} \tag{9}$$

Let us choose $\lambda_a = 0.3$, which corresponds to the mean value of the set to which $\lambda(t)$ belongs.

The gains $k_{1,aw}$ and $k_{2,aw}$ of this anti-windup device are tuned according to a low gain strategy as exposed in Lin (1998). For the considered parameter-varying application they were chosen as $k_{1,aw} = 0.1$ and $k_{2,aw} = 0.7$. Next, the global closed-loop system is discretized and the saturation is replaced by a deadzone operator. The following fourth-order system is then obtained:

$$\begin{aligned} \xi_{k+1} &= \underbrace{\begin{pmatrix} 1 & \tau & 0 & 0 \\ -\tau\lambda_k & 1-0.3\tau & 0.2\tau & -0.4\tau \\ 0 & 0 & 1 & \tau \\ 0 & 0 & -0.1\tau & 1-0.7\tau \end{pmatrix}}_{A_k} \xi_k + \underbrace{\begin{pmatrix} 0 \\ \tau L \\ 0 \\ \tau L \end{pmatrix}}_{B_k} \phi(v_k) \\ v_k &= \underbrace{\begin{pmatrix} \lambda_k L^{-1} & 0.3L^{-1} & -0.2L^{-1} & 0.4L^{-1} \end{pmatrix}}_{C_k} \xi_k \end{aligned} \tag{10}$$

with $\xi = [\xi_1 \ \ \xi_2 \ \ \xi_{1,aw} \ \ \xi_{2,aw}]'$ and where $\phi(.)$ denotes the standard, normalized deadzone operator and τ is the sampling time.

2.3 A preliminary simulation-based analysis

A preliminary simulation-based analysis of the above system is now performed with the initial condition $\xi_0 = [0 \ \ 2 \ \ 0 \ \ 0]'$ and $\tau = 0.3$.

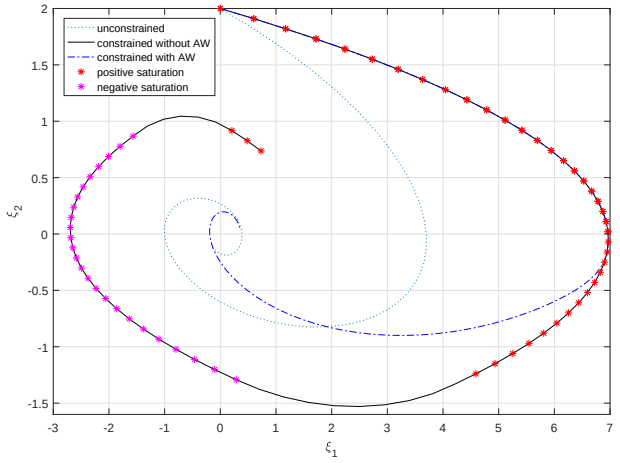

Fig. 2. A preliminary simulation-based analysis: phase portraits illustration.

Phase portraits are plotted in Figure 2 where the discrete-time values λ_k of the varying parameter starting from 0.1 are computed according to equation (5). The effect of the anti-windup system (whose response is visualized by the dash-dotted line) is clearly visible. The phase-portrait trajectory is indeed very close to the origin at the end of the considered horizon $[0\ N]$ for which $\lambda_N = 0.5$ and the control system is about to switch to the flare mode. Without anti-windup device, it is observed that the acceleration remains saturated (switching from L to $-L$) on large portions of the trajectory.

The next plots, visualized in Figure 3, show the evolution of $\|\xi\|$, the norm of the state vector as a function of time for the same three configurations as above (unconstrained, constrained without anti-windup and constrained with anti-windup). From this simulation, it can be concluded for the given initial state, that the vision-based control system, equipped with the anti-windup filter, is able to precisely track the glide slope trajectory despite a limited vertical acceleration capacity.

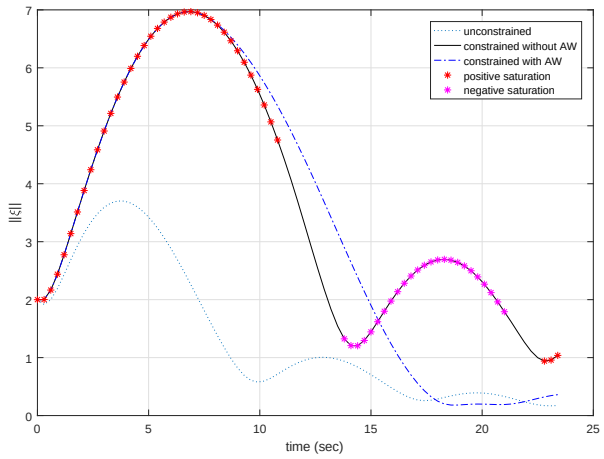

Fig. 3. A preliminary simulation-based analysis: time-domain results

However, the above simulation results do not provide any guarantees at least for different initial conditions. The remainder of the paper is then devoted to the evaluation of a guaranteed performance level without intensive simulations.

3. FINITE-TIME PERFORMANCE ANALYSIS RESULTS

Extending the infinite-horizon and continuous-time analysis results of Biannic and Burlion (2017) to a finite-time horizon analysis, the core of this paper is based on the study of discrete-time saturated LTV systems. The main result, presented next in Theorem 1 generalizes to the bounded horizon and time-varying case a previous result of Gomes da Silva Jr. and Tarbouriech (2006).

3.1 Main result

Theorem 1. (Finite-Time Performance of a Discrete-Time Saturated LTV System). Consider the discrete-time saturated LTV system, defined on the **bounded-horizon** $\{0, 1, \ldots, N\}$ by:

$$\begin{cases} \xi_{k+1} &= A_k\xi_k + B_k\phi(z_k)\,,\ k = 0\ldots N \\ z_k &= C_k\xi_k \end{cases} \tag{11}$$

where $\phi(.)$ denotes a normalized deadzone function. If there exist a set of positive definite matrices $Q_k \in \mathbb{R}^{n\times n}$, a set of diagonal matrices $S_k \in \mathbb{R}^{m\times m}$, a set of matrices $Z_k \in \mathbb{R}^{m\times n}$ and a positive real r such that:

$$\begin{pmatrix} Q_{k+1} & A_kQ_k & B_kS_k \\ Q_kA_k' & Q_k & Z_k' \\ S_kB_k' & Z_k & 2S_k \end{pmatrix} > 0\,,\quad k = 0\ldots N \tag{12}$$

$$\begin{pmatrix} Q_k & Z_k' + Q_kC_k' \\ Z_k + C_kQ_k & 1 \end{pmatrix} > 0\,,\quad k = 0\ldots N \tag{13}$$

$$Q_0 > \xi_0\xi_0' \tag{14}$$

$$Q_N < \rho I \tag{15}$$

then, any trajectory ξ_k of system (11) starting from the ellipsoidal set $\mathcal{E}_0$ that contains the initial vector ξ_0:

$$\mathcal{E}_0 = \{\xi \in \mathbb{R}^n / \xi' Q_0^{-1} \xi \leq 1\} \ni \xi_0 \tag{16}$$

will verify:

$$\xi_k \in \mathcal{E}_k,\ i.e.\ \xi_k'\, Q_k^{-1}\, \xi_k \leq 1\,,\quad k = 1\ldots N \tag{17}$$

and

$$\|\xi_N\| < \sqrt{\rho} \tag{18}$$

□

Sketch of proof: This theorem is easily established with the help of a time-varying quadratic Lyapunov function $V_k = \xi_k' P_k \xi_k$. The matrix inequality (12) in which $Q_k = P_k^{-1}$ clearly implies: $V_{k+1} < V_k$. The same auxiliary variables S_k et Z_k as those introduced in the continuous-time case Biannic and Burlion (2017) are used. This variables are a direct consequence of the use of the modified sector condition originally proposed by Gomes da Silva Jr. and Tarbouriech (2005). The set of inequalities (13) are also linked to the sector conditions and the same formulation is observed in the continuous-time case. The inequality (14) enforces the inclusion of the initial state vector ξ_0

inside the ellipsoidal set $\mathcal{E}_0$. One has indeed: $\xi_0' P_0 \xi_0 < 1 \Leftrightarrow Q_0 > \xi_0 \xi_0'$. Finally, the last inequality (15) $Q_N < \rho I$ also reads $P_N > \rho^{-1} I$, from which one obtains $\xi_N' \xi_N = \|\xi_N\|^2 < \rho . \xi_N' P_N \xi_N$. The result claimed by inequality (18) stems from the following fact: $V_N = x_N' P_N x_N < 1$ since, by assumption, $V_0 \leq 1$ and also from (12) which implies $V_{k+1} < V_k$. ■

3.2 Numerical complexity and resolution aspects

From a numerical viewpoint, the results stated in Theorem 1 are of high practical interest since they correspond to the minimization of the positive scalar ρ (i.e a linear objective) under linear matrix inequalities (LMI) constraints. However, both the number of constraints:

$$N_c = 2(N+2) \tag{19}$$

and the number of scalar decision variables:

$$N_v = 1 + (1 + \frac{n}{2})(1+n)(1+N) \tag{20}$$

may grow rapidly with the order n of the plant and the number of samples N. At the expense of precision, the latter (N) can be slightly reduced to some extent by increasing the sampling time. But the main options are based on relaxation strategies detailed next.

Reduction in the number of variables. The best option to limit complexity in the LMI optimization problem involved in Theorem 1 is to reduce the number of variables. This is rather easily performed here since the time-varying system matrices depend on a scalar parameter λ. The inequalities (12)- (15) can thus be rewritten:

$$\begin{pmatrix} Q(\lambda_{k+1}) & \star & \star \\ Q(\lambda_k)A'(\lambda_k) & Q(\lambda_k) & \star \\ S(\lambda_k)B'(\lambda_k) & Z(\lambda_k) & 2S(\lambda_k) \end{pmatrix} > 0\,, \quad k = 0 \dots N \tag{21}$$

$$\begin{pmatrix} Q(\lambda_k) & \star \\ Z(\lambda_k) + C(\lambda_k)Q(\lambda_k) & 1 \end{pmatrix} > 0\,, \quad k = 0 \dots N \tag{22}$$

$$Q(\lambda_0) > \xi_0 \xi_0' \tag{23}$$

$$Q(\lambda_N) < \rho I \tag{24}$$

and the variables can be chosen, for example, as polynomial functions with respect to λ. Let n_p denote the order of such polynomials, the total number of scalar decision variables now reduces to:

$$N_v = 1 + (1 + \frac{n}{2})(1+n)(1+n_p) \tag{25}$$

Reduced number of constraints. A trivial approach to reduce the number of constraints consists in increasing the sampling time in the discretization process to decrease N. This is however infeasible without a possibly significant loss of accuracy. Based on the above characterization, using parameterized functions, there is yet a possible alternative which consists in gridding the parameter space. Then, in inequalities (21) and (22), the index k will no longer evolve in the set $\{0, 1, \dots, N\}$ but in a much smaller subset $\{i_0, i_1, \dots, i_{N_r}\}$ such that $i_0 = 0$, $i_{N_r} = N$ and of course $N_r \ll N$. As a result, the number of constraints reduces to:

$$N_c = 2(N_r + 2) \tag{26}$$

The validity of the inequalities (21) and (22) on the entire set must however be checked *a posteriori* on the initial set and additional constraints must then be considered in case of failure which leads to a (possibly time-consuming) iterative process...

A specialized algorithm for affine parametrically dependent systems. As it can be noticed from equation (10), the state-space data $A_k = A(\lambda_k)$, $B_k = B(\lambda_k)$ and $C_k = C(\lambda_k)$ of the considered time-varying system depend affinely [1] on the parameter λ at each sampling time. In the context of LMI optimization, such a property is useful to guarantee that a parameter-dependent inequality holds by only testing the vertices of the parametric domain. This property forms the basis of the following algorithm with which both the number of variables (without using polynomial expressions) and the number of constraints can be simultaneously limited. As proposed above the algorithm is essentially based on a selection of sampling times:

$$\mathcal{I}_R = \{i_0, i_1, \dots, i_{N_r}\} \tag{27}$$

with $i_0 = 0$ and $i_{N_r} = N$. Next, for each interval $I_k = [i_k \; i_{k+1}]$ (with $k = 0 \dots N_r - 1$), piecewise constant Lyapunov functions $V_k = x_k' P_k x_k$ and relaxation variables Z_k and S_k are used. Then, the $2(N+2)$ inequalities (21)-(24) become:

$$\begin{pmatrix} Q_k & \star & \star \\ Q_k A'(\lambda_{i_k}) & Q_k & \star \\ S_k B'(\lambda_{i_k}) & Z_k & 2S_k \end{pmatrix} > 0\,, \quad k = 0 \dots N_r - 1 \tag{28}$$

$$\begin{pmatrix} Q_k & \star & \star \\ Q_k A'(\lambda_{i_{k+1}-1}) & Q_k & \star \\ S_k B'(\lambda_{i_{k+1}-1}) & Z_k & 2S_k \end{pmatrix} > 0\,, \quad k = 0 \dots N_r - 1 \tag{29}$$

$$\begin{pmatrix} Q_{k+1} & \star & \star \\ Q_k A'(\lambda_{i_{k+1}}) & Q_k & \star \\ S_k B'(\lambda_{i_{k+1}}) & Z_k & 2S_k \end{pmatrix} > 0\,, \quad k = 0 \dots N_r - 1 \tag{30}$$

$$\begin{pmatrix} Q_k & \star \\ Z_k + C(\lambda_{i_k})\, Q_k & 1 \end{pmatrix} > 0\,, \quad k = 0 \dots N_r - 1 \tag{31}$$

$$\begin{pmatrix} Q_k & \star \\ Z_k + C(\lambda_{i_{k+1}})\, Q_k & 1 \end{pmatrix} > 0\,, \quad k = 0 \dots N_r - 1 \tag{32}$$

$$Q_0 > \xi_0 \xi_0' \tag{33}$$

$$Q_{N_r} < \rho I \tag{34}$$

Remark 2. Since an affine parametric dependence is assumed here, the above inequalities, by a standard convexity argument, imply that (21) and (22) are satisfied with $Q(\lambda) = Q_k$, $S(\lambda) = S_k$ and $Z(\lambda) = Z_k$ if $\lambda \in [i_k \; i_{k+1}[$.

Algorithm 1. Finite time performance analysis of affine parametrically dependent systems.

(1) Define a subset $\mathcal{I}_R = \{i_0, i_1, \dots, i_{N_r}\}$
(2) Solve the LMI optimization problem:
$$\min \rho \;/\; (28), (29), (30), (31), (32)$$
(3) Go back to step (1) and update $\mathcal{I}_R$ to possibly reduce ρ otherwise stop the algorithm.

Remark 3. The number of constraints and variables involved in the above algorithm are respectively reduced to:

$$N_c = 5N_r + 2 \tag{35}$$

and

$$N_v = 1 + (1 + \frac{n}{2})(1+n)N_r \tag{36}$$

Remark 4. The use of a piecewise constant Lyapunov function possibly leads to conservative results when there

[1] Note that $B(\lambda_k)$ is even a constant, but this additional property will not be exploited in the proposed algorithm.

are not enough points in the selected subset. In such as case, as is proposed in Algorithm 1, a new (denser) set must be provided at the expense of a higher computational burden. An alternative option consists of using piecewise affine functions:

$$Q(\lambda) = \frac{\lambda_{k+1} - \lambda}{\lambda_{k+1} - \lambda_k} Q_k + \frac{\lambda - \lambda_k}{\lambda_{k+1} - \lambda_k} Q_{k+1} \qquad (37)$$

with $\lambda \in [\lambda_k \ \lambda_{k+1}]$. In this case the matrix inequalities (28)-(32) are now second-order polynomials in λ and must then be checked a posteriori to establish their validity for each interval I_k. An efficient alternative option to ensure their validity a priori can also be proposed with the help of additional constraints to enforce a multi-convexity property (see Apkarian and Tuan (2000)).

4. APPLICATION TO THE VISION-BASED LANDING ANALYSIS PROBLEM

The proposed finite-time performance characterizations are now applied to evaluate the vision-based landing system detailed in Section 2. The total order of the system including anti-windup augmentation is limited to $n = 4$. Moreover, the studied horizon is bounded by $T = 25\,s$ and N is thus no larger than 80 (with sampling time $\tau = 0.3\,s$). For these moderate dimensions, the main result stated by Theorem 1 is directly applicable. As emphasized in equations (19) and (20), the LMI problem to be solved involves around 160 constraints and 1200 decision variables.

The results of the application of Theorem 1 are visualized in Figure 4. The problem is solved iteratively over increasing time horizons T_i from $3\,s$ to $24\,s$. In each case, a guaranteed upper-bound $\rho(T_i)$ (visualized by a magenta star) is computed as well as an ellipsoidal set of initial conditions that includes ξ_0. As in subsection 2.3, the latter is fixed to $\xi_0 = [0 \ 2 \ 0 \ 0]'$. The lower-bound, represented by the blue solid line curve is simply obtained by the discrete-time trajectory starting from the initial condition ξ_0.

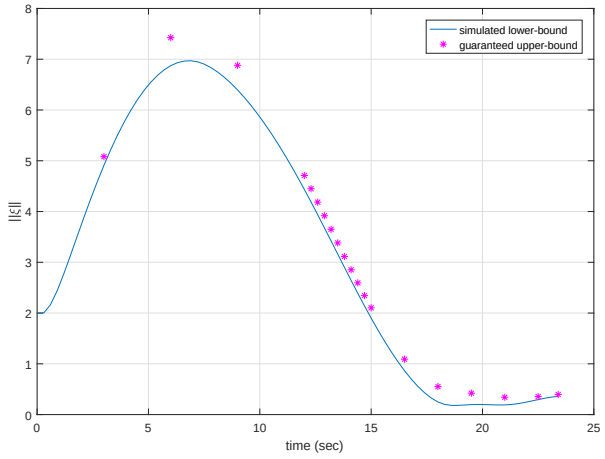

Fig. 4. Finite-time performance analysis: a simulated lower-bound and guaranteed upper-bounds

As one could expect, the conservatism of the proposed characterization in Theorem 1 is reasonably low. At the end of the studied horizon, the gap between upper and lower bounds is very tight indeed and the analysis technique thus captures the beneficial effects of the anti-windup system after $15\,s$. Unfortunately, this approach is limited to moderate dimensions problems. The computational burden may however be significantly reduced with the help of Algorithm 1 which has also been applied on the same study case for various subset $\mathcal{I}_R$ with growing size. The results are summarized in Table 1.

N_r	10	20	30	Theorem 1
N_c	62	102	152	160
N_v	166	316	466	1196
ρ	infeasible	1.89	0.478	0.396

Table 1. Application of Algorithm 1

The good compromise between accuracy and computational complexity is obtained here with $N_r = 30$. Note that for this choice, the number of constraints is not significantly reduced in comparison with theorem 1. However the number of variables is much smaller. As suggested in Remark 4, less conservative results can be obtained with piecewise affine functions.

5. CONCLUSION AND FUTURE WORK

New performance analysis results have been presented in this paper for time-varying saturated systems over a bounded horizon. The proposed characterization has been successfully tested to evaluate the performance of a landing system with an anti-windup loop. Thanks to well-chosen relaxation techniques the computational complexity can be limited which makes the proposed approach applicable to higher order systems than those considered in this paper. Moreover, extensions (possibly using the IQC framework as proposed in Fry et al. (2017); Seiler et al. (2017)) may also be investigated to introduce robustness aspects with respect to parametric uncertainties. On the application level, more complex vision-based landing control systems, including the flare phase, will also be studied with similar tools in a near future.

REFERENCES

Apkarian, P. and Tuan, H. (2000). Parameterized LMIs in Control Theory. *SIAM Journal on Control and Optimization*, 38(4), 1241–1264.

Azinheira, J. and Rives, P. (2008). Image-based visual servoing for vanishing features and ground lines tracking: Application to a uav automatic landing. *International Journal of Optomechatronics*, 2, 275–295.

Biannic, J.M. and Burlion, L. (2017). Performance analysis of saturated parameter-varying systems with application to vision-based landing assessment. In 20^{th} *IFAC World Congress*. Toulouse, France.

Bourquardez, O. and Chaumette, F. (2007). Visual servoing of an airplane for auto-landing. In *Proceedings of the IEEE/RSJ International Conference on Intelligent Robots and Systems*. San Diego, CA, USA.

Burlion, L. and de Plinval, H. (2017). Vision based anti-windup design with application to the landing of an Airliner. In 20^{th} *IFAC World Congress*. Toulouse, France.

Dickmanns, D., Boada, J., Gibert, V., and Schubert, F. (2015). Vision based landing for commercial aircraft. In *Proceedings of the 6th European Conference for Aeronautics and Space Sciences*. Krakow, Poland.

Dorato, P. (1961). Short time stability in linear time-varying systems. In *Proceedings of IRE International Convention Record, Part 4.*, 83–87.

Fry, J., Farhood, M., and Seiler, P. (2017). IQC-based robustness analysis of discrete-time linear time-varying systems. *International Journal of Robust and Nonlinear Control*, 27(16), 3135–3157.

Garcia, G., Tarbouriech, S., and Bernussou, J. (2009). Finite-Time Stabilization of Linear Time-Varying Continuous Systems. *IEEE Transactions on Automatic Control*, 54(2), 364–369.

Gibert, V., Burlion, L., Chriette, A., Boada, J., and Plestan, F. (2015). Vision based automatic landing of a civil aircraft by using nonlinear pose estimation. In *Proceedings of the 6th European Conference for Aerospace Sciences*. Krakow, Poland.

Gibert, V. and Puyou, G. (2013). Landing of an airliner using image-based visual servoing. In *9th IFAC Symposium on nonlinear control systems*. Toulouse, France.

Gomes da Silva Jr., J. and Tarbouriech, S. (2005). Anti-windup design with guaranteed regions of stability: An LMI-based approach. *IEEE Transactions on Automatic Control*, 50(1), 106–111.

Gomes da Silva Jr., J. and Tarbouriech, S. (2006). Anti-windup design with guaranteed regions of stability for discrete-time linear systems. *Systems & Control Letters*, 55, 184–192.

Huh, S. and Shim, D. (2010). A vision-based automatic landing method for fixed-wing uavs. *Journal of Intelligent and Robotic Systems*, 57, 217–231.

Le Bras, F., Hamel, T., Barat, C., and Mahony, R. (2009). Nonlinear image-based visual servo controller for automatic landing guidance of a fixed-wing aircraft. In *Proceedings of the European Control Conference*. Budapest, Hungary.

Lin, Z. (1998). *Low Gain Feedback*. Springer, Berlin, New-York, London.

Seiler, P., Moore, R., Meissen, C., Arcak, M., and Packard, A. (2017). Finite horizon robustness analysis of LTV systems using integral quadratic constraints. *CoRR*. URL `http://arxiv.org/abs/1711.07248`.

Zaccarian, L. and Teel, A. (2011). *Modern Anti-Windup Synthesis*. Princeton University Press.